University of South Carolina
Scholar Commons

Faculty Publications | Electrical Engineering, Department of

11-2000

High Performance Micropane Electron Beam Window

Roger A. Dougal
University of South Carolina - Columbia, dougal@engr.sc.edu

Shengyi Liu
Boeing, shengyi.liu@boeing.com

Follow this and additional works at: https://scholarcommons.sc.edu/elct_facpub

Part of the Electrical and Computer Engineering Commons

Publication Info

Published in *Journal of Vacuum Science and Technology B*, Volume 18, Issue 6, 2000, pages 2750-2756.
http://avspublications.org/jvstb/
© 2000 by the American Institute of Physics

This Article is brought to you by the Electrical Engineering, Department of at Scholar Commons. It has been accepted for inclusion in Faculty Publications by an authorized administrator of Scholar Commons. For more information, please contact dillarda@mailbox.sc.edu.

High performance micropane electron beam window

Roger A. Dougal[a] and Shengyi Liu
Department of Electrical and Computer Engineering, University of South Carolina, Columbia, South Carolina 29208

(Received 8 June 2000; accepted 28 August 2000)

A silicon disk etched so that it contains a multitude of microscopic and thin window panes (micropanes) can potentially transmit a larger average electron beam current density and absorb a smaller fraction of the beam energy than a common metal foil window. The enhanced performance is achieved by a combination of decreased power loss due to the extremely small window thickness (~1 μm), and increased conductive cooling due to the small diameter (~50 μm) of the micropanes and the large cross section of the honeycomb structure that supports the micropanes. Beam current densities up to 34 A/cm^2 are permitted within each micropane. When integrated over many micropanes across the face of a window, average current densities up to 1 A/cm^2 are permitted—at least three orders of magnitude larger than the <mA/cm^2 typical of foil windows. The small mass thickness yields high transparency, even for low energy beams. The transmission efficiency for a 100 keV beam is 99.5. © *2000 American Vacuum Society.* [S0734-211X(00)04506-6]

I. INTRODUCTION

Plasma source or field emission electron beams are used in a variety of manufacturing processes including surface modification,[1] material joining and cutting,[2] medical equipment sterilization,[3] polymerizing and cross linking of polymers,[4,5] and waste treatment.[6–8] The utility and electrical efficiency of electron beam sources are, in many cases, hampered by the means to extract the beam from the vacuum region in which it is created to the ambient environment in which it performs work. Electron beam windows of two types are currently used: differentially pumped orifices[9,10] and thin foils (metal or polymer).[11] Each of these has noteworthy disadvantages.

A differentially pumped orifice, as shown in Fig. 1(a), requires a substantial vacuum pumping system with high volumetric throughput. The large vacuum pumps require a significant capital outlay, regular maintenance, and large energy expenditure to keep running. Such windows are practical only in well-focused systems in which the orifice diameter can be kept small to minimize the required pumping speed.

Thin foils as shown in Fig. 1(b) are, on the other hand, essentially maintenance free and cheap, but suffer from their own disadvantages. They dissipate a significant fraction of the electron beam energy,[11] they are fragile, and the cost associated with window failure is often quite high.[12] Foil windows are typically made from Al or Ti. A thickness of only 15–50 μm withstands 1 atm of pressure. Despite that very thin cross section, beams having kinetic energies lower than ~100 keV cannot even penetrate the foil. At 100 keV, energy loss is 20% for an Al foil of 20 μm thickness, and nearly 40% for a Ti foil of the same thickness. The fraction of power lost in the foil is inversely proportional to the beam energy. Energy loss in the foil has important ramifications regarding system efficiency, but more seriously, it limits the average power density that can be transported through the foil at any cost. This power density limit often results in an engineering solution such as scanning the beam across a large-area foil[13] located at the end of a scan horn so as not to overheat any one location. Such solutions obviously do not work for cutting and drilling applications where high stationary power densities are required, and they are undesirable due to the increased risk of failure associated with the large foil area.

In some applications, it is possible to flow a thin film of water over a foil window to increase the heat extraction rate.[14] As a result of the reduced thermal load, the foil can be made thinner. The water film absorbs some of the beam energy, though, so the overall efficiency of this system is still limited (20% loss), and the presence of the water film restricts this technique to some particular applications. More recently, foil windows with built-in hydraulic cooling microchannels were described.[15] By creating a turbulent flow in capillary tubing within the window (eliminating the open-water interface), the absorbed energy can be effectively removed, and the beam current density can be increased by several orders of magnitude. Since the foil thickness is limited by the size of the microchannels (130 μm), this essentially eliminates its use in applications requiring low beam energy. Moreover, one expects considerable scattering of the beam, a high manufacturing cost, and complications from the adjunct plumbing system.

A particular problem with most beam windows is low efficiency for beams of low energy. But such low energy beams are desirable in many instances, often because low energies enable the system to be self-shielded.[16] This protects workers (and equipment) from the x radiation produced by beam interactions with the solid materials.

We describe here a new concept in electron beam window design which can greatly increase the energy efficiency and compactness of electron beam sources. It is ideally suited for use with microtip field emission sources,[17] since it passes an array of collinear beamlets. The micromachined silicon win-

[a]Electronic mail: Dougal@ece.sc.edu

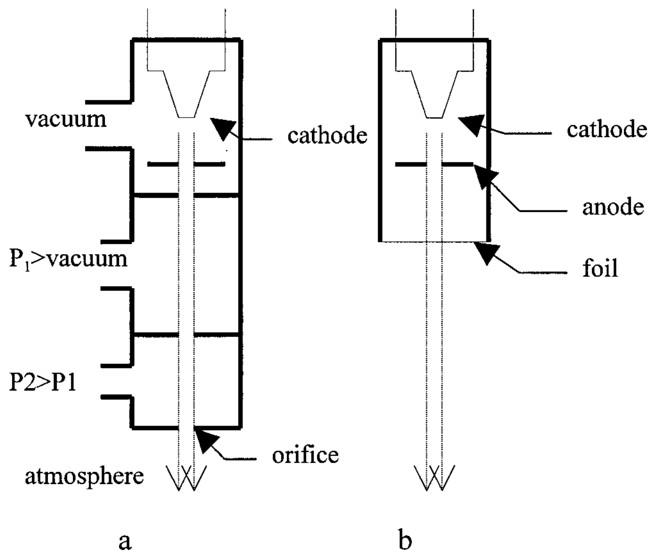

FIG. 1. Electron beam window based on (a) differentially pumped orifice, and (b) foil window.

dow, shown in Fig. 2, contains a multiplicity of very small and very thin window elements (the term *micropane* will be used here), each micropane being substantially thinner than is possible for a typical metal foil window. This new design exhibits substantially higher performance than existing designs for a number of reasons. First, the very thin micropane absorbs little energy from the electron beam. Second, the material parameters (strength, thermal conductivity, etc.) of silicon allow higher operating temperatures and stresses within the micropane. Third, the thick cross section of the honeycomb structure surrounding the micropanes gives more strength to the entire window and allows more efficient heat removal from the micropanes. The cumulative result of these improvements is a 1000-fold improvement in window performance.

The new window design eliminates a majority of the shortcomings of either type of traditional electron beam window. Cumbersome vacuum pumps can be eliminated from the electron beam source, window reliability is enhanced, and window size is reduced. The window is ideally suited for

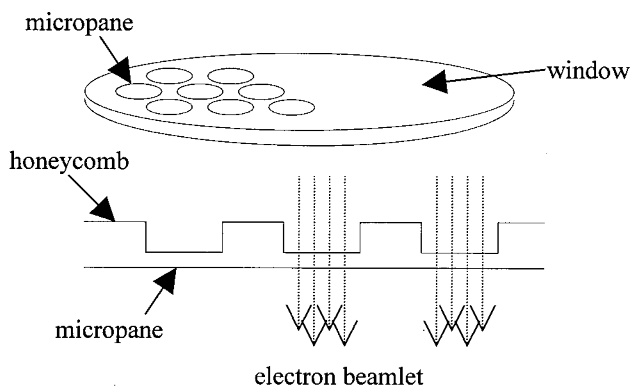

FIG. 2. Micromachined silicon electron beam window contains many micropanes etched into the window wafer, leaving a supporting honeycomb structure for strength and heat conduction.

TABLE I. Mechanical properties of window materials.

		Aluminum	Titanium	Silicon
Density	(g/cm^3)	2.70	4.54	2.33
Atomic weight	(AMU)	27	47.9	28
Melting point	(K)	933	1933	1683
Specific heat	(J/g K)	0.90	0.52	0.71
Thermal conductivity	(W/cm K)	2.36	0.2	1.18
Thermal expansion	(%/C)	25×10^{-6}	8.5×10^{-6}	3×10^{-6}
Tensile strength	(dyne/cm^2)	3.0×10^{9}	7.6×10^{9}	7.0×10^{9}
Young's modulus	(dyne/cm^2)	7×10^{11}	11×10^{11}	11×10^{11}
Yield strength	(dyne/cm^2)	0.17×10^{10}	0.43×10^{10}	7×10^{10}

materials processing applications that require a diffuse beam (flue gas treatment, polymerization and cross linking of plastics, etc.), but also, electron optics can be added to produce a focused beam for pointwise irradiation applications such as welding.

II. WINDOW PERFORMANCE

The micromachined silicon windows offer superior performance for the following reasons:

(1) the high melting point allows operation at high temperatures,
(2) good material strength withstands larger stress,
(3) the thin micropane section absorbs little energy,
(4) the honeycomb structure provides high physical strength, and
(5) the honeycomb structure offers high thermal conductivity.

The material properties of the common electron beam window materials, Al and Ti, are compared to those of silicon in Table I. Virtually all of the material properties of Si are superior to those of Al and comparable to those of Ti for this application. The density of silicon is lower than that of either competing element (almost half that of titanium), thereby giving a lower electron beam stopping power per unit thickness, and a concomitantly lower beam scattering coefficient. The melting point of silicon vastly exceeds that of aluminum so the window can operate at a higher temperature. The thermal conductivity is much higher than that of Ti, so heat can be more rapidly extracted from the window. The coefficient of linear expansion is significantly smaller than for the other materials, so thermal gradients will cause lower internal thermal stresses. The yield strength is significantly higher and the Young's modulus approximately the same as that of the other materials. The ease with which silicon can be machined by microelectronic etching processes is then fortuitous, considering that virtually all of its other properties are also superior to those of alternate window materials.

These qualitative arguments imply that micropane silicon windows may be substantially better than existing electron beam exit windows. A powerful motivation for using the micromachined silicon window is to decrease the fraction of beam energy lost in the window. A more precise quantifica-

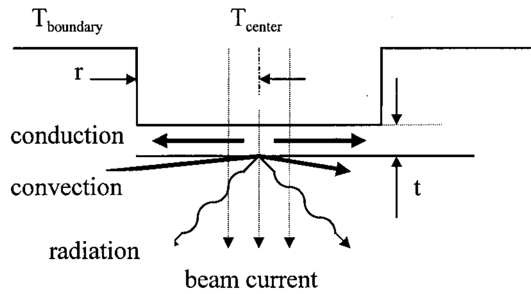

FIG. 3. Three mechanisms for heat extraction from a window foil.

tion of the benefits follows in the next section where we consider the power transmission capability of a generic window of circular configuration.

III. ANALYSIS

Consider first a thin window foil of thickness t and radius r bounded by a strong frame that also serves as a perfect heat sink, as shown in Fig. 3. Heat energy deposited in the foil by the beam can be removed by three routes—by conduction through the foil to the frame, by convection from the air side of the window, or by radiation from both sides of the window. The contributions of each of these processes will be examined in detail.

At a beam energy E (measured in electron volts) and current density J, the specific power P (W/cm^2) absorbed by a thin foil (i.e., one that absorbs a small fraction of the electron beam energy) of thickness t and mass density ρ, to a first approximation, can be evaluated through the Thomson–Whiddington law[18]

$$P=Jt\frac{\rho\chi}{2E}\frac{Z}{A}\quad(\mathrm{W/cm^2}),\tag{1}$$

where Z/A is the ratio of atomic number to atomic mass of the material, and χ is an energy loss coefficient having value 7.7×10^{11} cm^2 g^{-1}. The energy deposited in the foil is inversely proportional to the kinetic energy of the beam and linearly proportional to the foil thickness.

It is thus desirable to make the foil as thin as possible consistent with strength adequate to withstand the pressure differential. The mechanical stress σ on a circular foil depends on the pressure differential p the foil radius r_0 and the thickness t according to

$$\sigma=p\frac{r_0^2}{t^2}\ (\mathrm{dyne/cm^2}).\tag{2}$$

For a given yield stress σ_{yield} and pressure differential, the minimum foil thickness depends on the diameter of the foil

$$t_{\min}=\sqrt{p\frac{r_0^2}{\sigma_{\mathrm{yield}}}}\ (\mathrm{cm}).\tag{3}$$

A foil of minimum thickness and uniform material properties, then absorbs a specific power:

$$P=\frac{J\rho\chi}{2E}\frac{Z}{A}\sqrt{p\frac{r_0^2}{\sigma_{\mathrm{yield}}}}\ (\mathrm{W/cm^2}).\tag{4}$$

The specific power loss in the foil scales linearly with the radius of the foil. This characteristic is used in the design strategy of the present micropane window. By reducing the radius of each micropane, the minimum thickness can be reduced, and power dissipation is thus minimized. A high-transmitted power flux is achieved by using multiple micropanes, as will be detailed later. The dissipated heat must be extracted from the window to prevent failure. The heat extraction rate depends on the thermal conductivity k of the foil, the geometry, and the temperature difference between the foil and the various heat sinks. In steady state, the foil absorbs precisely the same amount of power as it dissipates by the cooling mechanism. Consider now a foil that absorbs a specific power P. If uniform convective cooling is the only mechanism, (no radiation and no thermal conduction to the frame) then the foil temperature will be essentially uniform across its surface and the foil will equilibrate at a temperature that satisfies

$$P=G(T_{\mathrm{window}}-T_{\mathrm{ambient}})\ (\mathrm{W/cm^2}),\tag{5}$$

where G is the convection cooling coefficient.

If instead uniform radiative cooling is the only cooling mechanism, then again the foil will equilibrate at a temperature described by

$$P=\sigma_{\mathrm{SB}}\epsilon(T_{\mathrm{window}}^4-T_{\mathrm{ambient}}^4)\ (\mathrm{W/cm^2}),\tag{6}$$

where σ_{SB} is the Stefan–Boltzmann coefficient and ϵ is the emissivity of the foil.

Finally, if conductive cooling is the only operative mechanism, then the temperature will increase monotonically towards the center and the difference in temperature between the center and the peripheral boundary will satisfy

$$P=\frac{(T_c-T_b)}{r_0^2}\cdot4kt\ (\mathrm{W/cm^2}).\tag{7}$$

Here, T_c is the temperature at the center and T_b is the temperature at the boundary.

Now, let us compare the magnitudes of the allowable specific powers that can be deposited in a foil cooled by each one of these various mechanisms while the peak temperature is limited to 1000 K above ambient.

(a) Convection coefficients for forced air cooling of smooth surfaces lie near 0.01 W cm^{-2} K^{-1}. For a 1000 K temperature differential between the foil and ambient, the convective cooling rate lies in the range of 10 W cm^{-2}. This is independent of the foil size.

(b) Radiative cooling rates depend on the emissivity of the material. For a typical emissivity of 0.1, and the same 1000 K temperature differential between the foil and ambient, the radiative cooling rate is approximately 1.6 W cm^{-2}. This is also independent of the foil size.

(c) Conductive cooling depends strongly on the foil dimensions r and t, and in this case the temperature is a function of position on the foil. We will take the standard 1000 K

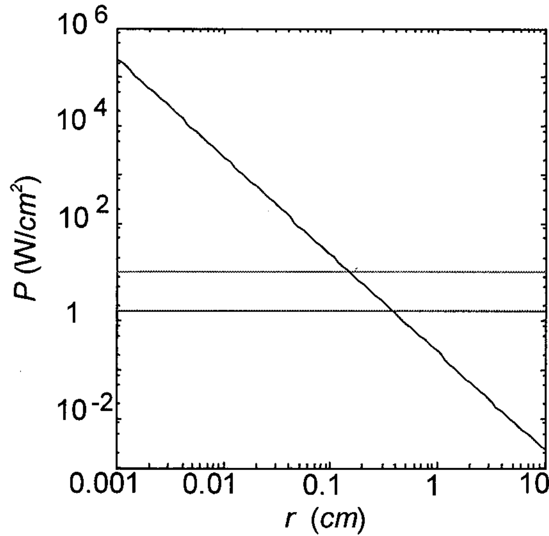

FIG. 4. Specific power deposition that produces a 1000 K temperature rise in a foil window for each of the three cooling mechanisms, as a function of window radius.

temperature differential to exist between the center of the foil and the foil boundary. The specific power that can be accepted by the foil depends inversely on the square of the foil radius and linearly on the foil thickness. For a common foil thickness of 10 μm and a thermal conductivity of 1 W cm^{-1} K^{-1}, conductive cooling allows a maximum specific power deposition of only 200 mW cm^{-2} for a foil of radius 5 cm but a phenomenal 47 kW cm^{-2} for a foil of 100 μm radius (for which the 10 μm thickness is actually excessively strong).

The power handling capacities for the three cooling modes are graphed as a function of window radius in Fig. 4. Note that traditional foil windows operate in the right half of the size domain shown in this figure, where the conductive cooling rate is orders of magnitude smaller than the radiative and convective cooling rates. Hence, the only way to increase transmitted power is to increase the foil area. The silicon micropane window, in comparison, operates in the left half of the size domain, where the conductive cooling rate is orders of magnitude larger than the other cooling rates.

The electron beam current that can be transmitted through a silicon micropane can be found by equating the power deposited in the micropane to the heat power that can be conducted through the micropane to the honeycomb. Consider first the idealized situation of a single micropane in a much thicker honeycomb that can be held at ambient temperature. Then

$$J\frac{\chi\rho}{2E}\cdot\frac{Z}{A}\sqrt{p\frac{r_0^2}{\sigma}}=(T_c-T_b)\frac{4k}{r_0^2}\sqrt{p\frac{r_0^2}{\sigma}}, \tag{8}$$

$$I=\pi r_0^2 J(\mathrm{A}), \tag{9}$$

$$I=\frac{8\pi E}{\chi\rho}\cdot\frac{A}{Z}k(T_c-T_b)\ (\mathrm{A}). \tag{10}$$

In the conductive cooling regime the current capacity for a single micropane is thus independent of the radius and thickness of the micropane! For silicon parameters, and assuming that $T_c-T_b=1000$ K, and a beam energy of 100 keV, the current limit is approximately 3.3 mA.

More current can then be carried by a window by increasing the number of micropanes in it (and decreasing the radius of the micropanes, if necessary). Thus, unlike foil windows, we have a means of increasing the average current density transported through the window, so long as the honeycomb structure itself can be adequately cooled.

For operation in the conductive cooling mode, the current capacity of a single micropane is independent of the micropane thickness because both the power deposited and the conductive cooling rate vary linearly with the thickness of the pane. On the other hand, the total heat power that must be conducted through the honeycomb to *its* surroundings is the sum of that deposited in all of the micropanes, so thin micropanes of small radius are desirable to maximize the total power transmission of the entire window. Thinness is also desirable to maximize transparency and to minimize beam scattering. In the conductive cooling regime, the current capacity is also independent of material yield strength. That is not the case for traditional foil windows where current capacity can only be added by increasing the window area and hence imposing larger strains.

The current capacity of a window containing many micropanes is now limited by heat transmission through the honeycomb. To determine the number of micropanes that a window can support before the heat loading in the honeycomb becomes excessive we consider the general form of the temperature profile across a window containing many micropanes, as shown in Fig. 5. We assume that conductive cooling dominates for the entire window now, rather than just for the micropane. The thicker (~400 μm) cross section of the honeycomb ensures that—even for windows up to several centimeters in diameter. (Convection and radiation will then only increase the current capacity of the window.) The temperature at the mounting flange will now be designated as T_f, and, in keeping with the earlier convention, T_b is the maximum temperature of the honeycomb at any micropane boundary and T_c is the maximum temperature at the center of any micropane (see Fig. 5).

Many variables can be traded off against each other to optimize the performance of the window. The allowable micropane thickness t, and hence the power absorption, decrease in direct proportion to the radius of the micropane. Simultaneously, the conductive cooling rate of the micropane increases as the micropane radius decreases. Hence, many small micropanes hold an advantage over a few larger micropanes of equivalent area. Too many micropanes per unit area decreases the effective conduction cross section and the strength of the honeycomb, so the micropane density must be limited. The total temperature rise from the flange to the center of the central micropane is limited by the melting point of the window material. The more of this temperature differential that is used up in the micropane (T_c-T_b), the

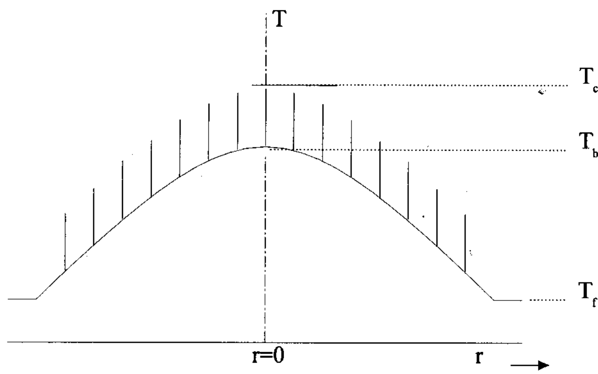

FIG. 5. Temperature profile across the window, assuming uniform average power dissipation over the window and uniform local power dissipation over each micropane.

less is available for conduction through the honeycomb to the flange $(T_b - T_f)$. Thus, for micropanes of a specific size, there must be an optimum density of such micropanes.

Differentiating the function that describes the power handling capacity of the window with respect to the micropane radius shows that the optimum micropane radius is zero. Since this is impractical, we should choose the smallest possible micropane radius according to other criteria such as manufacturability, ease of directing an electron beamlet through the micropane, and so forth. We will take these numbers here to be $t = 1\ \mu$m and $r_0 = 50\ \mu$m.

We now estimate the maximum power handling capacity of a micromachined silicon window containing a large number of micropanes. The specific power that can be absorbed by any individual micropane and then conducted to the honeycomb is [repeating Eq. (7)]

$$P_{\text{pane}} = \frac{(T_c - T_b)}{r_0^2} \cdot 4kt\ (\text{W/cm}^2). \tag{11}$$

At a micropane density of n_p (No./cm^2) the specific power dissipated in the window is

$$P_{\text{win}} = P_{\text{pane}} n_p \pi r_0^2 = (T_c - T_b) \cdot 4\pi k t n_p\ (\text{W/cm}^2). \tag{12}$$

The specific power that can be absorbed by the window and conducted through the window to the flange [modifying Eq. (7) appropriately] is

$$P_{\text{win}} = \frac{(T_b - T_f)}{R^2} \cdot 4kt_w\ (\text{W/cm}^2), \tag{13}$$

where R is the window radius. Equating (11) and (12) yields the honeycomb temperature T_b as

$$T_b = \frac{T_f + T_c(R^2 \pi n_p t/t_w)}{(1 + R^2 \pi n_p t/t_w)}(\text{K}). \tag{14}$$

For the parameters $R = 1$ cm, $t = 1\ \mu$m, $t_w = 400\ \mu$m, $n_p = 100/\text{cm}^2$, $T_f = 300$ K, and $T_c = 1500$ K, the peak temperature T_b at the center of the window (at the central micropane boundary) is 960 K. This corresponds to a specific power absorption of 120 W/cm^2 for the window as a whole, or a dissipation in each micropane of approximately 1.2 W. The specific power dissipation in each micropane is approximately 16 kW/cm^2. For micropanes of 50 μm radius, 1 W of power dissipation corresponds to transmission of 3 mA of current at a beam energy of 100 keV. A window of 1 cm radius (with 100 micropanes/cm^2) is then capable of transporting a total current of 870 mA, or an average current density of 280 mA/cm^2. This greatly exceeds the current capacity of foil windows. Simultaneously, the thinner cross section absorbs considerably less of the beam energy, making the transmission efficiency at least 99.5%.

IV. FURTHER ANALYSIS

The Thomson–Whiddington law used in the preceding analysis conveniently relates energy loss to the window properties (thickness, material, etc.);[19] its simplicity makes the analysis both easy and straightforward. For thin foils the Thomson–Whiddington (TW) law is a good approximation, but it does not reveal the detailed collision processes or electron number transmission efficiency. In what follows, we validate our use of the TW law by comparing the final results to those obtained from a semiempirical formula obtained by Monte Carlo simulation and experimental data.

The energy deposition by an electron beam propagating through matter is described by the collision stopping power, or depth-dose distribution function.[20] For a thin foil, each individual electron deposits its energy via multiple collisions before leaving the foil, or it may lose its energy completely and be thermalized. Thus, the transmitted energy can be described by the product of the average energy of the transmitted electrons and the number transmission efficiency of electron[21]

$$E_{\text{tr}}(x) = E_0 \exp\left[-a_1 \frac{x}{x_0} - a_2 \left(\frac{x}{x_0}\right)^{1-a_3}\right] \exp\left[-\alpha \left(\frac{x}{x_0}\right)^{\beta}\right] \text{eV}, \tag{15}$$

where a_1, a_2, a_3, x_0, α, and β are constants depending on the foil materials and the beam initial energy. E_0 is the initial energy in electron volts. The product of the first two factors in Eq. (15) is the average energy of the transmitted electrons, and the third factor is the number transmission efficiency. A comparison of Eq. (15) to the TW law is graphically shown in Fig. 6 for an initial energy of 100 keV and a silicon foil. The TW law yields higher transmitted energy due to its assumption of 100% number transmission efficiency, but the discrepancy is only 3% for a 10 μm thick foil, and 0.1% for a 1μm foil (a typical value for silicon micropane).

The specific power absorbed by a foil of thickness t at the beam current density J is

$$P_{\text{ab}}(t) = J \cdot E_{\text{ab}}(t)/e(\text{W/cm}^2), \tag{16}$$

where

$$E_{\text{ab}}(t) = E_0 - E_{\text{tr}}(t)\ (\text{eV}) \tag{17}$$

is the absorbed energy and e is the electron charge. In steady state, the amount of power absorbed is completely removed by conduction cooling, therefore the current density is, using Eqs. (2) and (7) in Eq. (16):

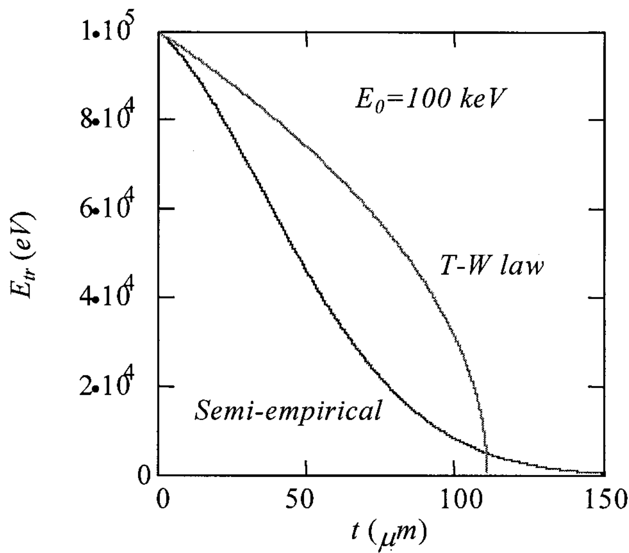

FIG. 6. Transmitted energies according to semiempirical relation (15) and Thomson–Whiddington law for an incident beam energy of 100 keV and a silicon foil.

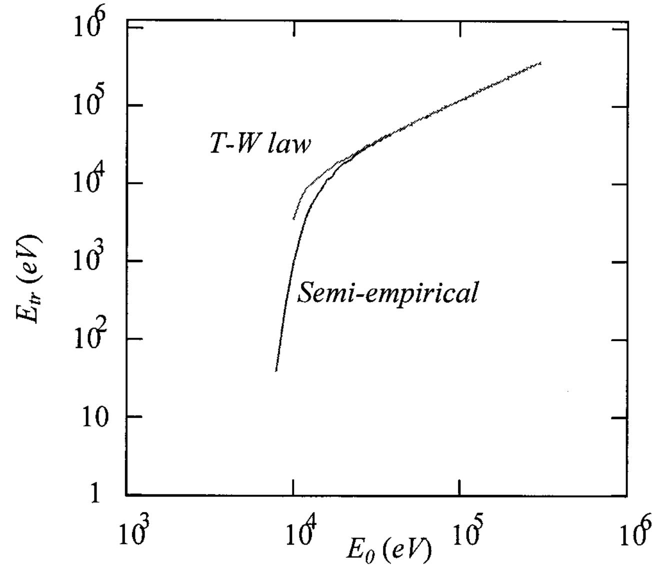

FIG. 8. Transmitted energy as a function of incident electron energy for 1 μm thick silicon window as computed according to the TW law and Eq. (15).

$$J(t)=\frac{4k(T_c-T_b)p}{\sigma\cdot t\cdot E_{\rm ab}(t)/e}\ ({\rm A/cm^2}). \tag{18}$$

Notice that the current density is inversely proportional to the product of the thickness and the absorbed energy. The total beam current allowed for each micropane, according to Eq. (18), can be calculated according to

$$I(t)=\pi r_0^2 J(t)=\frac{T_c-T_b}{E_{\rm ab}(t)/e}\cdot 4\pi kt\ ({\rm A}). \tag{19}$$

A comparison of the current described by Eq. (19) to that described by the TW law is given in Fig. 7 for an initial beam energy of 100 keV and a silicon foil. As the thickness increases, the allowed current decreases according to Eq. (19), but it remains constant according to the earlier derivation based on the TW law. At $t=1$ μm, the current is 2.7 mA from Eq. (19), about 0.6 mA lower than calculated from Eq. (10).

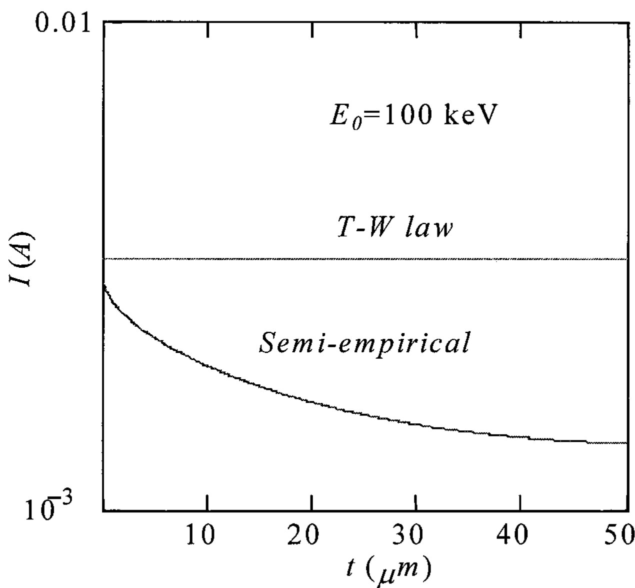

FIG. 7. Limiting current as a function of window thickness calculated from Eq. (19) and from Thomson–Whiddington law for an incident beam energy of 100 keV and a silicon foil.

Equation (18) defines the current density at critical mechanical stress—that is, where the mechanical stress equals the yield strength. In a practical design, the mechanical stress can be made much smaller than the yield strength by reducing the radius of the micropane window, which has the side effect of raising the allowed current density substantially. For example, for a micropane thickness of $t=1$ μm the mechanical stress limit $\sigma=\sigma_{\rm yield}$ allows a window radius $r_0=265$ μm. For a micropane of that size, the current density is 1.21 A/cm^2 (which is quite a respectable number). But for a more conservative mechanical design with parameters $t=1$ μm and $r_0=50$ μm, where the mechanical stress is $\sigma=2.5\times10^9$ dyne/cm^2 (well below the yield strength $\sigma_{\rm yield}=7\times10^{10}$ dyne/cm^2) the allowed current density is 33.9 A/cm^2, 28 times higher. A similar design property is also demonstrated by Eq. (4) or (8), from which a decreasing power loss or an increasing current density is obtained for a smaller window radius. This shows the effectiveness of using the TW law in the design strategy.

It is worthwhile to compare the energy response of a silicon micropane window as described by Eq. (15) to that described by the TW law. In Fig. 8, the transmitted energy is plotted as a function of the incident energy for a silicon foil of 1 μm thickness. For initial energies greater than 100 keV, both approaches give a transfer rate of nearly 100%. For both approaches, the rate drops below 50% for an initial energy of 50 keV, and the difference between the two approaches is less than 1%.

Finally, it is necessary to consider the effects of thermal

stress on the design. For a first approximation, the thermal stress is analyzed separately from mechanical stress. That is, the differential pressure is assumed zero, but a thermal stress exists due to a temperature gradient and a mechanical constraint at the boundary. For uniform energy deposition, the temperature distribution as a function of the radial distance r from the center of the micropane can be found as

$$T(r)=(T_c-T_b)\left(1-\frac{r^2}{r_0^2}\right)+T_b(\mathrm{K}), \quad (20)$$

where $r_0=50\ \mu\mathrm{m}$ is the radius of the micropane, $T_c=1300$ K is the temperature at the center, and $T_b=300$ K is the temperature at the micropane boundary. Thermal stresses arise due to the thermal gradient and because the thermal expansion is constrained at the boundary. Analysis of the plane–stress problem indicates that the maximum thermal stresses, located at the center of the micropane, have magnitude[22]

$$(\sigma_{\mathrm{th}})_{\max}=\sigma_{rr}(0)=\sigma_{\theta\theta}(0)=\alpha\cdot Y\left(\frac{1}{2}T(0)+\frac{1+v}{(1-v)r_0^2}\int_0^{r_0} rT(r)dr\right)\times(\mathrm{dyne/cm^2}), \quad (21)$$

where $\alpha=3\times10^{-6}\ \mathrm{K}^{-1}$ is the thermal expansion coefficient, $Y=11\times10^{11}\ \mathrm{dyne/cm^2}$ is the Young's modulus, and $v=0.35$ is Poisson's ratio. Using Eqs. (20) in Eq. (21) yields $(\sigma_{\mathrm{th}})_{\max}=4.89\times10^9\ \mathrm{dyne/cm^2}<\sigma_{\mathrm{yield}}$. Because the micropane design effectively minimizes the energy loss or the thermal load, both the thermal stress and the mechanical stress are much smaller than the yield strength.

V. SUMMARY

The micropane window is a dramatic improvement over traditional foil and pumped aperture windows now in use. It can transport a much higher current density, making it suitable for application in electron beam welders and heat treatment systems, and it absorbs much less energy from the beam, thereby dramatically increasing the electrical efficiency of electron beam sources, especially at relatively low beam energies.

This window scheme obviously requires an electron beam source that projects a multiplicity of small radius beamlets. A natural choice for the cathode is an array of field emission sources of the spindt type[17] where clusters of emitter arrays match the micropane topology. Field emission arrays (with tip spacing as small as 1 μm) offer locally averaged current densities large enough to take full advantage of the transmission capability of the micropane window. Together with accelerating and focusing electrodes (to collimate and direct the beamlets through the micropanes), a very compact 100 kV electron beam source is possible. Magnetic shielding will be required to prevent magnetic fields from deviating the beamlets, lest the beam miss the micropanes and the window be melted.

Several issues remain to be investigated. One potential problem is erosion of the micropanes by kinetic processes—electron impact or ion impact (on the atmospheric side of the window). A second possibility is chemical reactivity between the window and the ion stream external to the window, leading either to window thinning or to window thickening that will produce additional heating and subsequent window failure. Finally, the use of microchannel cooling within the web of the micropane should be explored.

[1] H. W. Bergmann, H. U. Fritsch, and G. Hunger, J. Mater. Sci. **16**, 863 (1981).
[2] *Introduction to Electron Beam Technology*, edited by R. Bakish (Wiley, New York, 1962).
[3] J. T. Allen *et al.*, Radiat. Phys. Chem. **46**, 457 (1995).
[4] A. Charlesby and V. Wycherley, Int. J. Appl. Radiat. Isot. **2**, 26 (1957).
[5] A Charlesby, *Atomic Radiation and Polymers* (Pergamon, London, 1960).
[6] M. R. Cleland, R. A. Fernald, and S. R. Maloof, Radiat. Phys. Chem. **24**, 179 (1984).
[7] K. Kawamura and T. Katayama, Radiat. Phys. Chem. **18**, 389 (1981).
[8] M. Nickelsen, W. Cooper, C. Kurucz, and T. Waite, Environ. Sci. Technol. **26**, 144 (1992).
[9] E. Gajdusek, Weld. J. (Miami) **59**, 17 (1980).
[10] Z. Zimek and R. A. Salimov, Radiat. Phys. Chem. **40**, 317 (1992).
[11] Yu. V. Grigor'ev and A. V. Stepanov, Instrum. Exp. Tech. **33**, 895 (1990).
[12] M. P. Simpson, *Impela News, Electron Beam Newsletter* **3**, Issue 2 (1996).
[13] L. G. Pittaway, Br. J. Appl. Phys. **15**, 967 (1964).
[14] M. N. Schuetz and D. A. Vroom, in *Environmental Applications of Ionizing Radiation*, edited by W. J. Cooper *et al.* (Wiley, New York, 1988), pp. 63–82.
[15] R. J. Vidmar and R. J. Barker, IEEE Trans. Plasma Sci. **26**, 1031 (1998).
[16] I. Sakamoto and Y. Hoshi, Radiat. Phys. Chem. **33**, 403 (1989).
[17] C. A. Spindt, C. E. Holland, A. Rosengreen, and I. Brodie, IEEE Trans. Electron Devices **38**, 2355 (1991).
[18] J. Vine and P. A. Einstein, Proc. IEEE **53**, 921 (1964).
[19] R. Whiddington, Proc. R. Soc. London, Ser. A **86**, 360 (1912).
[20] S. M. Seltzer and M. J. Berger, Int. J. Appl. Radiat. Isot. **33**, 1189 (1982).
[21] T. Tabata, R. Ito, and S. Tsukui, CCC-430, Radiation Shielding Information Center, Oak Ridge National Laboratory (1992); also appeared in Radiat. Phys. Chem. **35**, 821 (1990).
[22] B. A. Boley and J. H. Weiner, *Theory of Thermal Stresses* (Wiley, New York, 1960), Chap. 9, pp. 288–291.